**Full title page**

# Differential Diagnosis of Uterine Smooth Muscle Tumors using Diffusion-Weighted Imaging: Correlations with the Apparent Diffusion Coefficient and Cell Density

Akiko Tasaki MD,[1)] Mina O Asatani MD, PhD,[1)] Hajime Umezu MD, PhD,[2)] Katsunori Kashima MD, PhD,[3)] Takayuki Enomoto MD, PhD,[3)] Norihiko Yoshimura MD, PhD,[1)] Hidefumi Aoyama MD, PhD[1)]

1) Department of Radiology, Niigata University School of Medicine, 1-757 Asahimachi-Dori, Chuo-Ku, Niigata 951-8510, Japan
2) Division of Pathology, Niigata University Medical and Dental Hospital, 1-757 Asahimachi-Dori, Chuo-Ku, Niigata 951-8510, Japan
3) Department of Obstetrics and Gynecology, Niigata University School of Medicine, 1-757 Asahimachi-Dori, Chuo-Ku, Niigata 951-8510, Japan

**Corresponding author:** Akiko Tasaki

Department of Radiology, Niigata University School of Medicine, 1-757 Asahimachi-Dori, Chuo-Ku, Niigata 951-8510, Japan. Tel: +81-25-227-2315. Fax: +81-25-227-0877.

E-mail: asat1002@med.niigata-u.ac.jp

Word count: 2920

**Running title**: Differential Diagnosis of Uterine Smooth Muscle Tumors using DWI: Correlations with the ADC and Cell Density

**Acknowledgements**

This study was partially supported by the Funding Program for World-Leading Innovative R&D

on Science and Technology (First Program) initiated by the Council for Science and Technology Policy of Japan, as well as a Grant-in Aid for Scientific Research (21591602) from the Japanese Society for the Promotion of Science.

**Blinded Manuscript**

Differential Diagnosis of Uterine Smooth Muscle Tumors using Diffusion-Weighted Imaging: Correlations with the Apparent Diffusion Coefficient and Cell Density

**Abstract**

**Purpose:** To investigate the utility of the apparent diffusion coefficient (ADC) in differentiating benign and malignant uterine smooth muscle tumors classified by signal intensity (SI) on T2-weighted imaging (T2WI), and diffusion-weighted imaging (DWI); and to determine the correlation between ADC and tumor cell density.

**Methods:** This retrospective study reviewed 168 lesions in 134 cases with pathologically confirmed uterine smooth muscle tumors, including 6 leiomyosarcomas and 3 smooth muscle tumors of uncertain malignant potential (STUMPs), and preoperative magnetic resonance imaging examinations performed between October 2009 and November 2012. T2WI and DWI were also performed for each subject. Tumors were then classified according to SI on T2WI and DWI relative to myometrial SI. The correlation between ADC and tumor cell density was also determined.

**Results:** In Group 1(high on both T2WI/DWI), mean ADC was significantly lower for leiomyosarcoma ($0.91\times10^{-3}$ $mm^2/s$) than for leiomyoma ($1.30\times10^{-3}$ $mm^2/s$; $p<0.05$), and mean cell density significantly higher for leiomyosarcoma (42.9%) than for leiomyoma (22.4%; $p<0.05$). A strong negative correlation was seen between ADC and tumor cell density in Group 1 (Spearman, $R=-0.72$; $p<0.05$).

**Conclusion:** ADC may help to differentiate benign from malignant uterine smooth muscle tumors, particularly tumors with high SI on T2WI and DWI.

**Keywords:** Leiomyoma; Leiomyosarcoma; DWI/ADC; Correlation; Cell density

## Introduction

Uterine smooth muscle tumors are one of the main indications for female pelvic imaging. Most uterine smooth muscle tumors are benign leiomyomas, which occur in 20–30% of women during their reproductive years [1]. Typical leiomyomas appear as well-demarcated hypointense masses on T2-weighted magnetic resonance (MR) images [1]. However, using standard imaging it may be difficult to distinguish leiomyomas from malignant tumors, because some leiomyomas show hyperintensity on T2-weighted imaging (T2WI) [1, 2]. Malignant tumors including leiomyosarcomas often show hyper to heterogenous signal intensity (SI) on T2WI because of correspondence to hemorrhage or necrosis[3]. Owing to the difficulties associated with transvaginal needle biopsy for uterine smooth muscle tumors, preoperative diagnosis is important.

Diffusion-weighted imaging (DWI) is an emerging technique used to visualize tissue characteristics based on the diffusion motion of water molecules, known as Brownian motion[4]. The utility of this technique has been established in the central nervous system, primarily for the diagnosis of acute stroke [5].

DWI can also provide quantitative measurement of the apparent diffusion coefficient (ADC), which is thought to be influenced by the nuclear-to-cytoplasmic ratio and cellular density in solid tissues [4]. ADCs for malignant tumors in various organs have been reported to be decreased as compared with those for normal tissues or benign lesions [6-8].

Several recent studies have reported the utility of DWI/ADC for differentiating benign from malignant myometrial tumors [9-12]. However, these studies did not compare ADCs with the results from histopathological specimens. To the best of our knowledge, it has not yet been determined whether or not ADC reflects cell density in

uterine smooth muscle tumors.

The purpose of this study was to investigate the utility of ADCs in differentiating benign from malignant uterine smooth muscle tumors classified by T2WI/DWI SI; and to determine the correlation between ADC and uterine smooth muscle tumor cell density.

## Materials and Methods

*Patients*

From October 2009 to November 2012, a total of 2097 MR imaging examinations of the uterus and ovaries were carried out at our institute. The present retrospective study, for which our institutional review board did not require approval, identified 168 lesions in 144 cases with pathologically confirmed uterine smooth muscle tumors. Ten cases of leiomyoma were excluded because of highly red degeneration (n=7) and the presence of lipoleiomyoma (n=3). The aim of this study was to evaluate the cell density of the tumors. So we had excluded red degenerations and lipoleiomyomas because they did not show enhancement. The remaining 168 lesions in 134 cases (mean age, 41.0 years; range, 25–84 years) were included in the present study. Preoperative MR imaging including DWI was performed in all cases. The mean period from MR imaging to surgery was 33.4 days (range, 0–133 days). Gonadotropin-releasing hormone agonist therapy was carried out in 80 patients (mean, 4.35 courses; range, 2–7 courses). All women who had GnRHa therapy were included, because it might not have a great effect on MRI. ( They didn't treat in particular from MRI to surgery.)

The final histopathological diagnosis was leiomyoma in 159 lesions (125 cases), smooth muscle tumor of uncertain malignant potential (STUMP) in three lesions (three cases)

and leiomyosarcoma in six lesions (six cases).

Mean leiomyoma size was 6.4 cm (range, 1.5–21 cm), and that of leiomyosarcoma was 13.6 cm (range, 5.6–28 cm). Final diagnosis was established on the basis of histopathological examination of 56 lesions (49 leiomyomas, two STUMPs and five leiomyosarcomas) obtained during hysterectomy, 111 lesions (110 leiomyomas and one STUMP) obtained by myomectomy, and core needle biopsy from one leiomyosarcoma.

*MR imaging*

Uterine MR imaging was carried out on 92 lesions using a 1.5-T superconductive MR unit (22 cases using a Signa HDx, General Electric, Milwaukee, WI, USA and 70 cases using an Achieva, Phillips Medical Systems, Best, the Netherlands) and on 76 lesions using a 3.0-T superconductive MR unit (Verio; Siemens, Erlangen, Germany). A 5- or 8-channel cardiac coil was utilized with the 1.5-T unit and a 32-channel cardiac coil with the 3.0-T unit. Hyoscine butylbromide (20 mg; Buscopan: Boehringer, Ingelheim, Germany) was used as an antiperistaltic agent before image acquisition to reduce motion artifacts.

Turbo-spin-echo T1-weighted imaging (T1WI) (repetition time, 480–940 ms; echo time (TE), 7–13 ms) in the axial plane and fast-spin-echo fat-suppressed T2WI (fsT2WI) (TR, 3000–6000 ms; TE, 69–96 ms) in the axial and oblique sagittal planes was performed for all patients. Prior acquisition of DWI (TR, 1200–10,000 ms; TE, 60–78 ms; flip angle, 90°), T1WI and fsT2WI were uniform with a section thickness of 4–8 mm, and an intersection gap of 1–2 mm. Gadolinium contrast-enhanced T1WI was performed after an intravenous injection of gadolinium based contrast agent at a dose of 0.2 mmol/kg.

DWI was acquired in the axial plane in all patients using a single-shot echo-planar imaging sequence with b-values of (0 and 800) s/mm$^2$ on 1.5-T MR imaging and (0 and 900) s/mm$^2$ on 3-T MR imaging. All images, including from DWI, were uniformed with a section thickness of 5 mm, no intersection gap and a field of view (FOV) of 350 mm. ADC maps were derived automatically on a pixel-by-pixel basis from DWIs according to the following equation: $D = -[\ln(S1)-\ln(S0)]/(b1-b0)$, where b0 and b1 represent the b-values of lower and higher values, respectively, and S0 and S1 are the SIs for these b-values.

To evaluate the feasibility of using ADC values obtained from three different MR systems, we conducted a phantom study. The phantom (90-401: Nikko Fines Company, Tokyo, Japan) was scanned with b values of 0 and 800 s/mm$^2$ on two 1.5-T MR units (Signa HDx, General Electric and Achieva, Phillips Medical Systems) and b values of 0 and 900 s/mm$^2$ on a 3.0-T MR unit (Verio; Siemens) to determine the influence of b-value on DWI; the same coil was used as that in the clinical examinations. ADCs were calculated and the correlations between MR units were examined. A strong correlation ($R \geq 0.98$; $p < 0.01$) was found among the MR units, with ADCs being almost identical for b values ≤1500 [13]. We then aggregated the results from the 3 MR units for further examination.

MR images were diagnosed according to the consensus of two board-certificated radiologists with 3 and 4 years of experience in gynecological MR imaging (A.T. and M.A), who were blinded to the pathological results.

Tumors were classified into one of four groups according to SI on T2WI and DWI as compared with the SI of the myometrium: Group 1, high SI on both T2WI and DWI; Group 2, high SI on T2WI and iso- to low SI on DWI; Group 3, iso- to low SI on T2WI

and high SI on DWI; and Group 4, iso- to low SI on both T2WI and DWI.

*ADC values*

With respect to quantitative analysis, one of the readers recorded the ADCs of each tumor by placing regions of interest (ROIs) on ADC maps, in all tumors with a solid area ≥50 $mm^2$ with reference to gadolinium enhanced T1WI. Tumor parts with hemorrhages or cystic changes were excluded because the purpose was to evaluate the cell density. DWI becomes unreliable if it contains hemorrhages [14, 15] or cystic part for accurate cell density evaluation. ADCs of three ROIs were calculated for each tumor and the mean ADC was used.

*Analysis of tumor cell density*

Histopathological results were evaluated by one pathologist. Analysis of tumor cell density was performed by utilizing a method essentially similar to that used by Sugahara et al.[16], Hatakenaka et al. [7] and Tamura et al.[17].

A position of the tumor's cross section was listed in a macroscopic image. With reference to it, the microscopic image was decided under the consensus of two radiologists.

Cell density was analyzed using the free Image J software from the National Institutes of Health. Two of the authors randomly chose 1 FOV for each tumor from each specimen, all of which had undergone hematoxylin and eosin (HE) staining. Microscopic images were then saved for analysis together with information on the diagnosis.

According to previous studies on correlations between tumor tissues and ADCs,

tumor cell density was calculated as follows: 1) microscopic images were randomly taken from different regions in each tumor specimen (Fig. 1a); 2) red, green and blue (RGB) color spread processing was performed on each image and the red image in which the cell nucleus was most marked was selected (Fig. 1b); and 3) a threshold was defined to extract tumor cell nuclei and, based on this threshold, cell density was calculated using Adobe Photoshop Elements 7.0 software (Adobe Systems, San Jose, CA, USA) (Fig. 1c).

*Statistical analysis*

Differences in ADC and cell density were compared in all tumors, and in Group 1 between leiomyosarcomas, leiomyomas and STUMPs, using the Mann–Whitney U test (IBM SPSS<Dr.SPSS Ⅱ>). Values of $p<0.05$ were considered as being statistically significant.

We then compared correlations between the ADC and cell density in all tumors, and within each group, using Spearman's rank correlation.

**Results**

Tumors consisted of 159 leiomyomas, three STUMPs and six leiomyosarcomas. Group 1 contained 37 tumors (29 leiomyomas, two STUMPs and six leiomyosarcomas); Group 2 contained two leiomyomas; Group 3 contained 31 tumors (30 leiomyomas and one STUMP); and Group 4 contained 98 leiomyomas. All leiomyosarcomas were classified into Group 1 (Table 1). Two cases of cellular leiomyoma were included as leiomyomas (Group 1).

Mean tumor size was 13.6 cm (range, 5.6–28 cm) for leiomyosarcomas, 6.43 cm

(range, 1.5–21 cm) for leiomyoma and 8.9 cm (range, 5.5–10.7 cm) for STUMPs (Table 2). The mean ADC was $0.91\times10^{-3}$ $mm^2/s$ (range, 0.70–1.44 $\times10^{-3}$ $mm^2/s$) for leiomyosarcomas, $1.14\times10^{-3}$ $mm^2/s$ (range, 0.61–2.00 $\times10^{-3}$ $mm^2/s$) for leiomyomas and $1.19\times10^{-3}$ $mm^2/s$ (range, 0.90–1.42 $\times10^{-3}$ $mm^2/s$) for STUMPs (Table 2).

Mean cell density was 42.95% (range, 6.2–58.1%) for leiomyosarcomas, 20.72% (range, 1.3–69.8%) for leiomyomas and 26.7% (range, 16.5–44.3%) for STUMPs (Table 2).

Among all tumor types, the mean ADC was significantly lower for leiomyosarcomas ($0.91\times10^{-3}$ $mm^2/s$) than for leiomyoma ($1.14\times10^{-3}$ $mm^2/s$; $p<0.05$), and the mean cell density was significantly higher for leiomyosarcomas (42.9%) than for leiomyomas (20.7%; $p<0.05$; Fig. 2). A weak negative correlation between ADC and tumor cell density was found in all tumors (Spearman R=-0.490; $p<0.05$; Fig. 4a). The mean ADC of leiomyoma, excluding cellular leiomyoma, was $1.15\times10^{-3}$ $mm^2/s$, significantly higher than that of leiomyosarcoma ($p=0.013$) and the mean cell density was 20.70%, again showing a significant difference ($p=0.018$).

In Group 1, the mean ADC was $1.30\times10^{-3}$ $mm^2/s$ (range, 0.75–2.00 $\times10^{-3}$ $mm^2/s$) in leiomyoma, and the mean ADC was significantly lower for leiomyosarcoma ($0.91\times10^{-3}$ $mm^2/s$) than for leiomyoma ($1.30\times10^{-3}$ $mm^2/s$; $p<0.01$). Mean cell density was 22.43% (range, 1.3–69.8%) in leiomyoma, significantly lower than that in leiomyosarcomas (42.9%; $p<0.05$; Fig. 3). Excluding cellular leiomyomas, the mean ADC for leiomyoma was $1.36\times10^{-3}$ $mm^2/s$, significantly higher than that for leiomyosarcoma ($p=0.002$), and mean cell density was 19.1%, significantly lower than that for leiomyosarcoma ($p=0.01$).

A strong negative correlation between the ADC and tumor cell density was found in

Group 1 (Spearman, R=-0.727; $p<0.05$; Fig. 4b). In Group 3, the mean ADC was $0.99\times10^{-3}$ $mm^2/s$ (range, 0.61–1.44 $\times10^{-3}$ $mm^2/s$), and mean cell density was 39.25% (range, 9.9–56.6%). A negative correlation was evident between ADC and tumor cell density (Spearman, R=−0.650; $p<0.05$; Fig. 4c). In Group 4, the mean ADC was $1.12\times10^{-3}$ $mm^2/s$ (range, 0.71–1.83 $\times10^{-3}$ $mm^2/s$), and no correlation was identified between the ADC and tumor cell density (Spearman, R=−0.20; $p<0.05$; Fig. 4d).

**Discussion**

The present study compared DWI/ADC and histopathological results in all target uteine smooth muscle tumors. Previous studies have reported correlations between DWI/ADC and quantitative cell density in gliomas [16] and breast tumors [6-8, 17], but to the best of our knowledge, this is the first study to evaluate correlations between the ADC and cell density in uterine smooth muscle tumors.

All six leiomyosarcomas exhibited high SI on both T2WI and DWI; all were classified into Group 1, in which the mean ADC was significantly lower for leiomyosarcoma than for leiomyoma ($p<0.01$). In addition, mean cell density was significantly higher for leiomyosarcoma than for leiomyoma in this group ($p<0.05$). Previous studies have reported decreased ADCs for malignant tumors relative to normal tissues or benign lesions in various organs [4, 18-20], and the present results are consistent with those findings. One of the strengths of the current study was that we evaluated ADC and quantitative cell density in all cases, confirming strong negative correlations, particularly in tumors showing high SI on both T2WI and DWI.

Some benign leiomyomas, such as edematous degenerations and cellular leiomyomas, may show hyperintensity on T2WI. Distinguishing such lesions from

malignant tumors on the basis of routine MR examination is often difficult [21]. Group 1 in the present study included two cases of cellular leiomyoma. Cellular leiomyoma is composed of densely cellular fascicles of smooth muscle with little intervening collagen [22]. This hypercellular nature and lack of collagenous tissue may contribute to increased signal intensity on T2WI [21]. On DWI, the increased cellularity may restrict water diffusion and thus decrease ADC [9, 10].

In our study, the ADCs for cellular leiomyoma were $0.92\times10^{-3}$ $mm^2/s$ and $0.75\times10^{-3}$ $mm^2/s$, and cell densities were 62.9% and 69.8%. The ADCs for cellular leiomyomas likely reflected the underlying cell densities.

The increased SIs on DWI and decreased ADCs were similar to those for malignant tumors. The ADCs for cellular leiomyoma and leiomyosarcoma overlapped in the present study, as in previous reports [9, 10], and this can be explained by the increased cell densities [9-11]. Consequently, differentiating between leiomyosarcoma and cellular leiomyoma based on DWI and ADC is difficult2 cases of cellular leiomyomas and 3/6 cases of leiomyosarcomas showed clear margins, and 3 out of 6 cases of leiomyosarcomas had irregular margins. Irregular margins may be useful for differentiating cellular leiomyomas from leiomyosarcomas as reported [3], but the ratio is around 50%, so it may be not necessarily so.

On the other hand, no significant correlation was seen between ADCs and cell densities in Group 4 (low SI on both T2WI and DWI). The low SI for leiomyoma on DWI is predictable because the signal of the abundant rich collagenous fibers present is too low to be picked up. This phenomenon is regarded as being similar to the T2blackout effect, in which hypointensity on DWI is caused by hypointensity on T2WI, with the result that the ADC is probably unreliable, particularly in tumors showing low

SI on both T2WI and DWI [14, 15].

ADCs have been calculated using DWI not only in the present study, but also in many previous studies based on a monoexponential equation using only 2-point b-values (with zero as the low b-value) in pelvic MR imaging for women [9-11, 15]. ADCs calculated using this approach consist of a mixture of perfusion and diffusion information. Some studies have reported ADCs using multiple b-values in various organs [17, 23-28]. According to the intravoxel incoherent motion (IVIM) DWI model, pure extravascular molecular diffusion and the microcirculation of blood within the capillaries (perfusion) can be separated using a biexponential decay function, providing additional parameters for characterization [4]. It is therefore necessary to use ADCs that have been calculated by means of a biexponential equation using multi b-values, including those of myometrial tumors.

The primary limitation of the present study was the small sample size for leiomyosarcomas, which might not accurately reflect the characteristics of this type of tumor. Also, there were only 2 cases of cellular leiomyomas in our study. If we were able to make a subgroup for cellular leiomyomas, then there probably would be significant differences between leiomyosarcomas and ordinary leiomyomas, statistically.Another limitation was the fact that the results from the three MR units that were used were aggregated for further examination. As strong correlations existed between ADCs from these units, we examined the results together. Finally, no examination using multi-parametric MR imaging was conducted. Owing to the difficulties in performing transvaginal needle biopsy in uterine smooth muscle tumors, preoperative differentiation is important. Use of IVIM DWI with multiple b-values or

MR spectroscopy, which provides metabolic information, is highly recommended[29, 30].

In conclusion, the present findings suggest that ADC may be helpful in differentiating between benign and malignant tumors of the uterine smooth muscle, particularly when the tumors show high SI on T2WI and DWI.

**References**


1. Hricak H, Tscholakoff D, Heinrichs L et al: **Uterine leiomyomas: correlation of MR, histopathologic findings, and symptoms**. *Radiology* 1986, **158**(2):385-391.
2. Togashi K, Ozasa H, Konishi I et al: **Enlarged uterus: differentiation between adenomyosis and leiomyoma with MR imaging**. *Radiology* 1989, **171**(2):531-534.
3. Sahdev A, Sohaib SA, Jacobs I et al: **MR imaging of uterine sarcomas**. *AJR American journal of roentgenology* 2001, **177**(6):1307-1311.
4. Le Bihan D, Breton E, Lallemand D et al: **MR imaging of intravoxel incoherent motions: application to diffusion and perfusion in neurologic disorders**. *Radiology* 1986, **161**(2):401-407.
5. Li TQ, Takahashi AM, Hindmarsh T et al: **ADC mapping by means of a single-shot spiral MRI technique with application in acute cerebral ischemia**. *Magnetic resonance in medicine : official journal of the Society of Magnetic Resonance in Medicine / Society of Magnetic Resonance in Medicine* 1999, **41**(1):143-147.
6. Guo Y, Cai YQ, Cai ZL et al: **Differentiation of clinically benign and malignant breast lesions using diffusion-weighted imaging**. *Journal of magnetic resonance imaging : JMRI* 2002, **16**(2):172-178.
7. Hatakenaka M, Soeda H, Yabuuchi H et al: **Apparent diffusion coefficients of breast tumors: clinical application**. *Magnetic resonance in medical sciences : MRMS : an official journal of Japan Society of Magnetic Resonance in Medicine*

2008, **7**(1):23-29.

8. Lyng H, Haraldseth O, Rofstad EK: **Measurement of cell density and necrotic fraction in human melanoma xenografts by diffusion weighted magnetic resonance imaging**. *Magnetic resonance in medicine : official journal of the Society of Magnetic Resonance in Medicine / Society of Magnetic Resonance in Medicine* 2000, **43**(6):828-836.

9. Tamai K, Koyama T, Saga T et al: **The utility of diffusion-weighted MR imaging for differentiating uterine sarcomas from benign leiomyomas**. *European radiology* 2008, **18**(4):723-730.

10. Takeuchi M, Matsuzaki K, Nishitani H: **Hyperintense uterine myometrial masses on T2-weighted magnetic resonance imaging: differentiation with diffusion-weighted magnetic resonance imaging**. *Journal of computer assisted tomography* 2009, **33**(6):834-837.

11. Namimoto T, Yamashita Y, Awai K et al: **Combined use of T2-weighted and diffusion-weighted 3-T MR imaging for differentiating uterine sarcomas from benign leiomyomas**. *European radiology* 2009, **19**(11):2756-2764.

12. Shimada K, Ohashi I, Kasahara I et al: **Differentiation between completely hyalinized uterine leiomyomas and ordinary leiomyomas: three-phase dynamic magnetic resonance imaging (MRI) vs. diffusion-weighted MRI with very small b-factors**. *Journal of magnetic resonance imaging : JMRI* 2004, **20**(1):97-104.

13. Ogura A, Hayakawa K, Miyati T et al: **Imaging parameter effects in apparent diffusion coefficient determination of magnetic resonance imaging**. *European journal of radiology* 2011, **77**(1):185-188.

14. Hiwatashi A, Kinoshita T, Moritani T et al: **Hypointensity on diffusion-weighted MRI of the brain related to T2 shortening and susceptibility effects**. *AJR American journal of roentgenology* 2003, **181**(6):1705-1709.

15. Maldjian JA, Listerud J, Moonis G et al: **Computing diffusion rates in T2-dark hematomas and areas of low T2 signal**. *AJNR American journal of neuroradiology* 2001, **22**(1):112-118.

16. Sugahara T, Korogi Y, Kochi M et al: **Usefulness of diffusion-weighted MRI with echo-planar technique in the evaluation of cellularity in gliomas**. *Journal of magnetic resonance imaging : JMRI* 1999, **9**(1):53-60.

17. Tamura T, Usui S, Murakami S et al: **Comparisons of multi b-value DWI signal analysis with pathological specimen of breast cancer**. *Magnetic resonance in medicine : official journal of the Society of Magnetic Resonance in Medicine / Society of Magnetic Resonance in Medicine* 2012, **68**(3):890-897.

18. Liu KF, Li F, Tatlisumak T et al: **Regional variations in the apparent diffusion coefficient and the intracellular distribution of water in rat brain during acute focal ischemia**. *Stroke; a journal of cerebral circulation* 2001, **32**(8):1897-1905.

19. Yamashita Y, Tang Y, Takahashi M: **Ultrafast MR imaging of the abdomen: echo planar imaging and diffusion-weighted imaging**. *Journal of magnetic resonance imaging : JMRI* 1998, **8**(2):367-374.

20. Charles-Edwards EM, deSouza NM: **Diffusion-weighted magnetic resonance imaging and its application to cancer**. *Cancer imaging : the official publication of the International Cancer Imaging Society* 2006, **6**:135-143.

21. Yamashita Y, Torashima M, Takahashi M et al: **Hyperintense uterine leiomyoma at T2-weighted MR imaging: differentiation with dynamic enhanced MR imaging and clinical implications**. *Radiology* 1993, **189**(3):721-725.

22. Smoot JS, Zaloudek C: **Myometrial and stromal lesions of the uterus**. *Clinics in laboratory medicine* 1995, **15**(3):545-573.

23. Liu C, Liang C, Liu Z et al: **Intravoxel incoherent motion (IVIM) in evaluation of breast lesions: Comparison with conventional DWI**. *European journal of radiology* 2013, **82**(12):e782-789.

24. Sumi M, Van Cauteren M, Sumi T et al: **Salivary gland tumors: use of intravoxel incoherent motion MR imaging for assessment of diffusion and perfusion for the differentiation of benign from malignant tumors**. *Radiology* 2012, **263**(3):770-777.

25. Shinmoto H, Tamura C, Soga S et al: **An intravoxel incoherent motion diffusion-weighted imaging study of prostate cancer**. *AJR American journal of roentgenology* 2012, **199**(4):W496-500.

26. Sala E, Kataoka MY, Priest AN et al: **Advanced ovarian cancer: multiparametric MR imaging demonstrates response- and metastasis-specific effects**. *Radiology* 2012, **263**(1):149-159.

27. Peters NH, Vincken KL, van den Bosch MA et al: **Quantitative diffusion weighted imaging for differentiation of benign and malignant breast lesions: the influence of the choice of b-values**. *Journal of magnetic resonance imaging : JMRI* 2010, **31**(5):1100-1105.

28. Sala E, Priest AN, Kataoka M et al: **Apparent diffusion coefficient and**

**vascular signal fraction measurements with magnetic resonance imaging: feasibility in metastatic ovarian cancer at 3 Tesla: technical development**. *European radiology* 2010, **20**(2):491-496.

29. Takeuchi M, Matsuzaki K, Harada M: **Preliminary observations and clinical value of lipid peak in high-grade uterine sarcomas using in vivo proton MR spectroscopy**. *European radiology* 2013, **23**(9):2358-2363.

30. McLean MA, Priest AN, Joubert I et al: **Metabolic characterization of primary and metastatic ovarian cancer by 1H-MRS in vivo at 3T**. *Magnetic resonance in medicine : official journal of the Society of Magnetic Resonance in Medicine / Society of Magnetic Resonance in Medicine* 2009, **62**(4):855-861.

**Figure legends**

Figure1. **:** Procedure for estimating cell density

To extract the nuclear area, a coarse microscopic image (**a**) was divided into three primary color images (red, green, blue: (**b**)) using Image J.

The red image was selected, and a threshold defined as the nuclear area was extracted (**c**).

Cell density (nuclei area/all area) was then calculated using Photoshop version 7.0.

Figure2. : ADC values and cell densities for all tumors.

Figure 3. : ADC values and cell densities in Group1.

Figure4. : Correlation between ADC value and cell density.

**a)** In all tumors, a weak negative correlation was shown with ADC and cell density ($R=-0.49$, $p<0.001$).

**b)** In Group 1, a strong negative correlation was shown ($R=-0.72$, $p<0.001$).

**c)** In Group 3, a strong negative correlation was shown ($R=-0.65$, $p<0.001$).

**d)** In Group 4, no significant correlation existed between ADC and cell density ($R=-0.20$, $p<0.05$).

Figure5. : Group 1: Leiomyosarcoma in a 36-year-old woman.

**a)** Axial T2WI showing a poorly demarcated signal-hyperintense mass in the uterus.

**c)** DWI with a b-value of 800 $mm^2/s$ showing high signal intensity.

**d)** The ADC is 0.88 $\times 10^{-3}$ $mm^2/s$.

**b)** Hematoxylin and eosin-stained specimen. The cell density is 47.4%.

Figure6. : Group 1; Benign leiomyoma in a 30-year-old woman.

**a)** Axial T2WI showing a well-demarcated signal-hyperintense mass in the subserosa.

**c)** DWI with a b-value of 900 $mm^2/s$ showing high signal intensity on the dorsal aspect of the tumor.

**d)** The ADC is 1.60 $\times 10^{-3}$ $mm^2/s$.

**b)** Hematoxylin and eosin-stained specimen. The cell density is 11.9 %.

Figure7. : Group 3: Leiomyoma in a 62-year-old woman.

**a)** Axial T2WI showing a well-demarcated signal hypointense mass in the myometrium.

**c)** DWI with a b-value of 800 $mm^2/s$ showing high signal intensity on the dorsal aspect of the tumor.

**d)** ADC is 0.88 $\times 10^{-3}$ $mm^2/s$.

**b)** Hematoxylin and eosin-stained specimen. The cell density is 45.4%.

Figure8. : Group 4; Ordinary leiomyoma in a 42-year-old woman.

**a)** Axial T2WI showing a well-demarcated signal hypointense mass in the myometrium and subserosa.

**c)** DWI with a b-value of 800 $mm^2/s$ showing low signal intensity.

**d)** The ADC is 1.21 $\times 10^{-3}$ $mm^2/s$.

**b)** Hematoxylin and eosin-stained specimen. The cell density is 19.4%.

Table 1: Tumors classified into the 4 groups

Group 1: High SI on both T2WI and DWI.

Group 2: High SI on T2WI, iso- to low SI on DWI.

Group 3: Iso- to low SI on T2WI, high SI on DWI.

Group 4: Iso- to low SI on both T2WI and DWI.

Table 2: ADC and cell density by histopathological results

**Table 1.** Tumors classified into the 4 groups.

| **Group** | **Histopathogical result** | **n** | | **total** |
|---|---|---|---|---|
| **1** | **LMS** | **6** | **37** | **168** |
| | **LM** | **29** | | |
| | **STUMP** | **2** | | |
| **2** | **LM** | **2** | | |
| **3** | **LM** | **30** | **31** | |
| | **STUMP** | **1** | | |
| **4** | **LM** | **98** | | |

Group 1: High SI on both T2WI and DWI.

Group 2: High SI on T2WI, iso- to low SI on DWI.

Group 3: Iso- to low SI on T2WI, high SI on DWI.

Group 4: Iso- to low SI on both T2WI and DWI.

**Table 2**, ADC and cell density by histopathological results

| **Histopathological results** | **n** | **diameter (mean ) cm** | **ADC value ( mean ) $\times 10^{-3}$ mm $^{2}$/sec** | **cell density ( mean )%** |
|---|---|---|---|---|
| **LMS** | **6** | **5.6 - 28 (13.6)** | **0.70 - 1.44 ( 0.91)** | **6.2 - 58.1 ( 42.95)** |
| **LM** | **159** | **1.5 - 21 ( 6.43)** | **0.61 - 2.00 ( 1.14)** | **1.3 - 69.8 ( 20.72)** |
| **STUMP** | **3** | **5.5 - 10.7 ( 8.9)** | **0.90 - 1.42 ( 1.19)** | **16.5 - 44.3 ( 26.7)** |

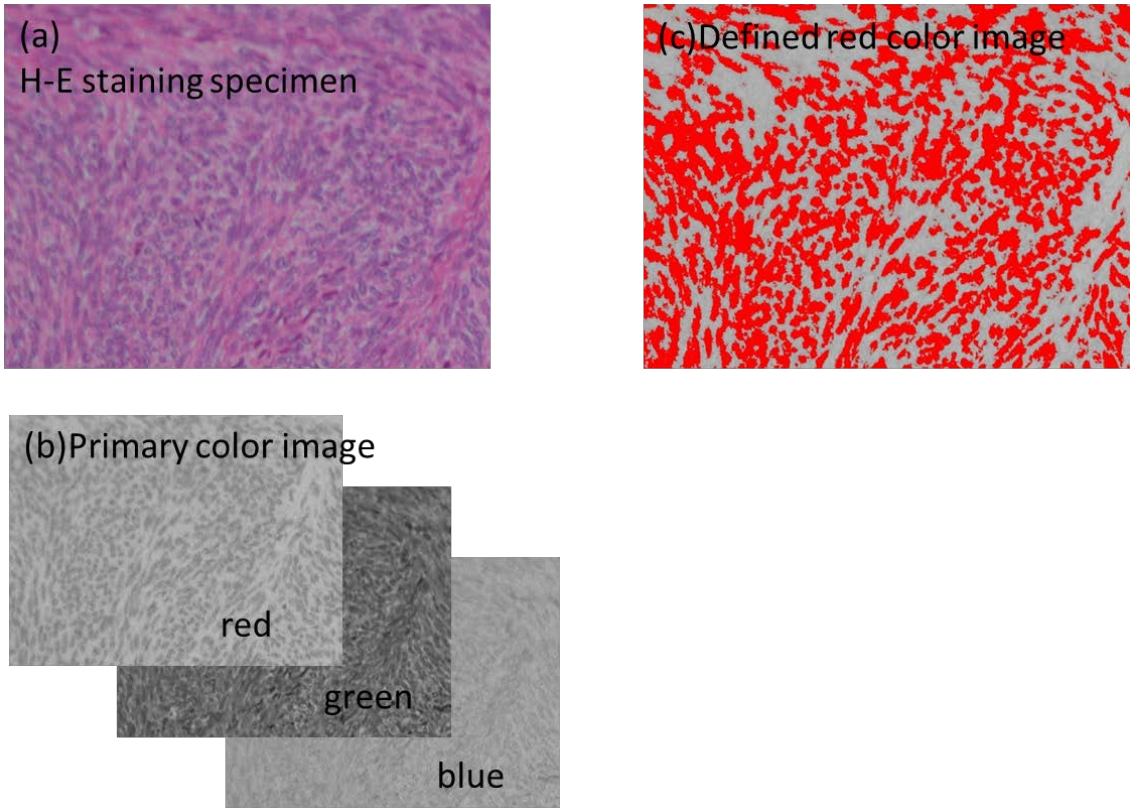


Figure1. **:** Procedure for estimating cell density

To extract the nuclear area, a coarse microscopic image (**a**) was divided into three primary color images (red, green, blue: (**b**)) using Image J.

The red image was selected, and a threshold defined as the nuclear area was extracted (**c**).

Cell density (nuclei area/all area) was then calculated using Photoshop version 7.0.

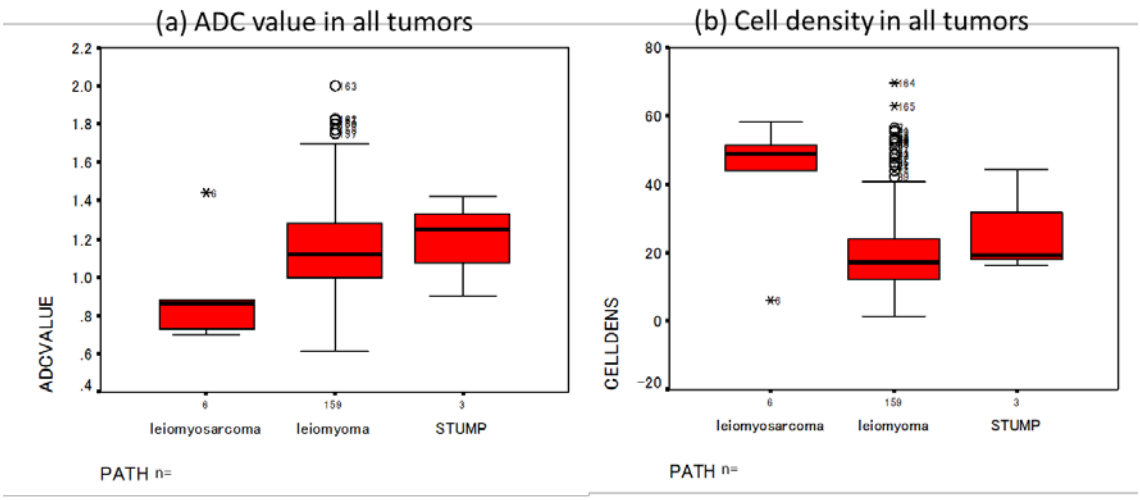


Figure2. : ADC values and cell densities for all tumors.

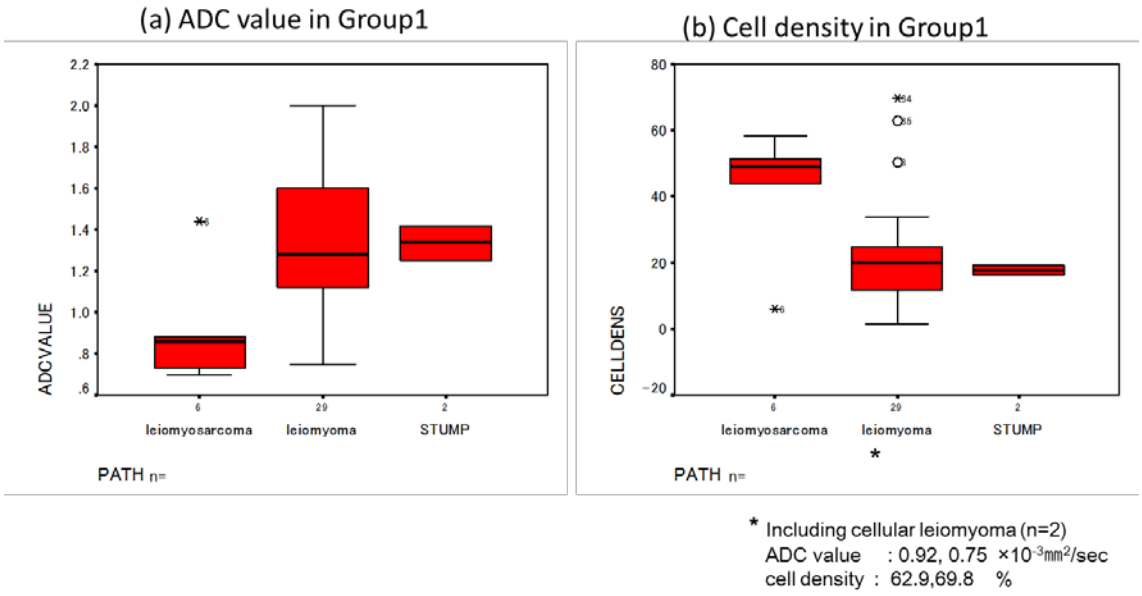


Figure 3. : ADC values and cell densities in Group1.

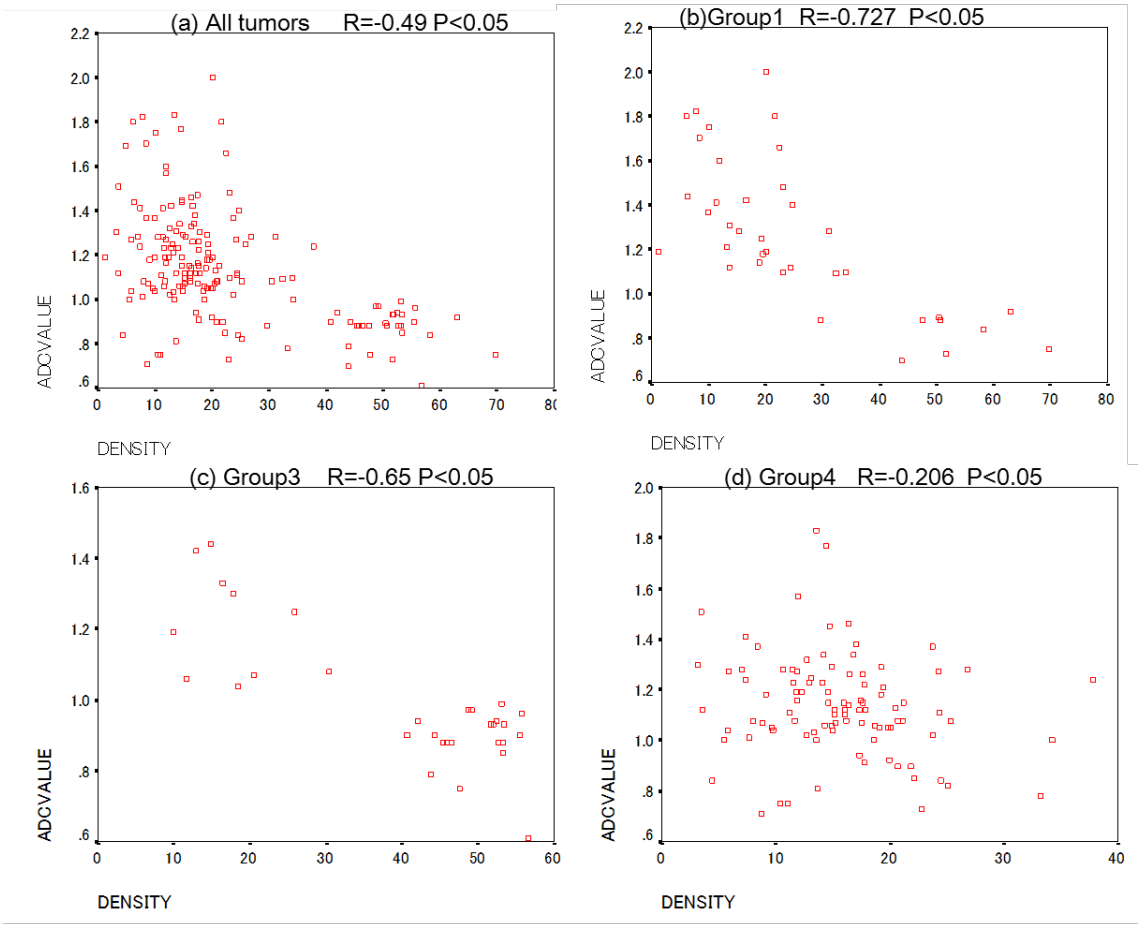


Figure4. : Correlation between ADC value and cell density.

**a)** In all tumors, a weak negative correlation was shown with ADC and cell density (R=-0.49, p<0.001).

**b)** In Group 1, a strong negative correlation was shown (R=-0.72, p<0.001).

**c)** In Group 3, a strong negative correlation was shown (R=-0.65, p<0.001).

**d)** In Group 4, no significant correlation existed between ADC and cell density (R=-0.20, p<0.05).

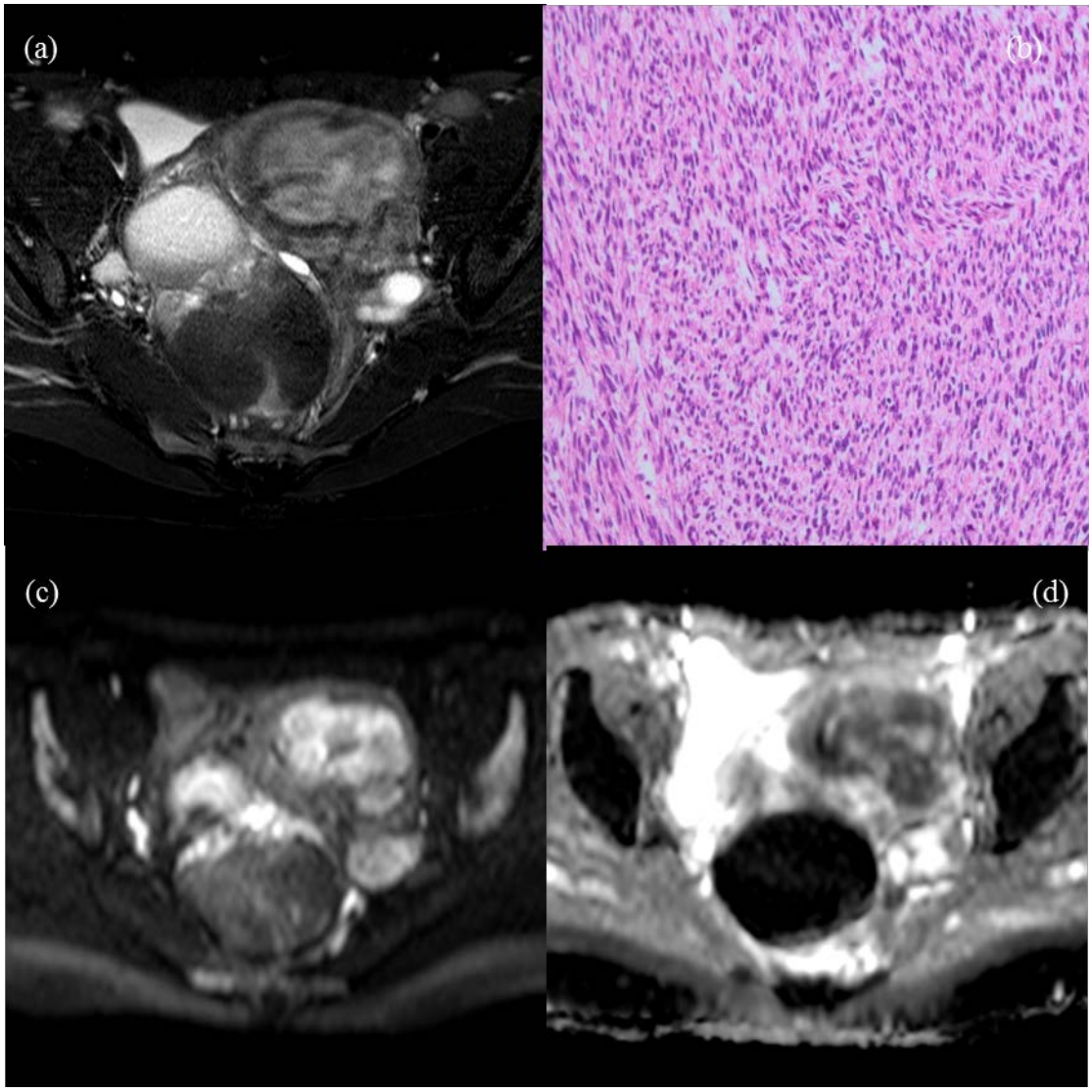


Figure5. : Group 1: Leiomyosarcoma in a 36-year-old woman.

**a)** Axial T2WI showing a poorly demarcated signal-hyperintense mass in the uterus.

**c)** DWI with a b-value of 800 $mm^2/s$ showing high signal intensity.22

**d)** The ADC is 0.88 $\times 10^{-3}$ $mm^2/s$.

b) Hematoxylin and eosin-stained specimen. The cell density is 47.4%.

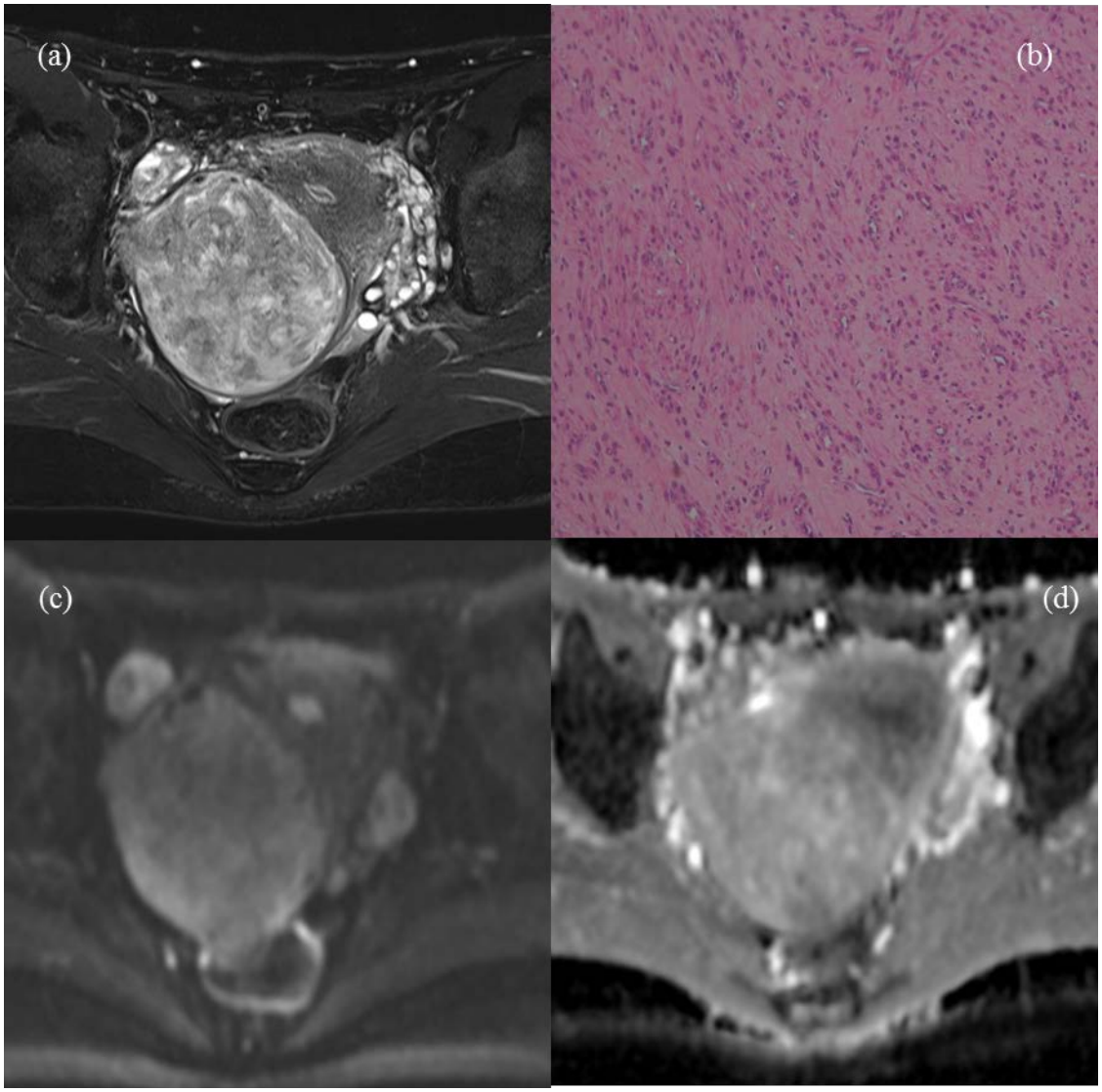


Figure6. : Group 1; Benign leiomyoma in a 30-year-old woman.

**a)** Axial T2WI showing a well-demarcated signal-hyperintense mass in the subserosa.

**c)** DWI with a b-value of 900 $mm^2/s$ showing high signal intensity on the dorsal aspect of the tumor.

**d)** The ADC is 1.60 $\times 10^{-3}$ $mm^2/s$.

b) Hematoxylin and eosin-stained specimen. The cell density is 11.9 %.

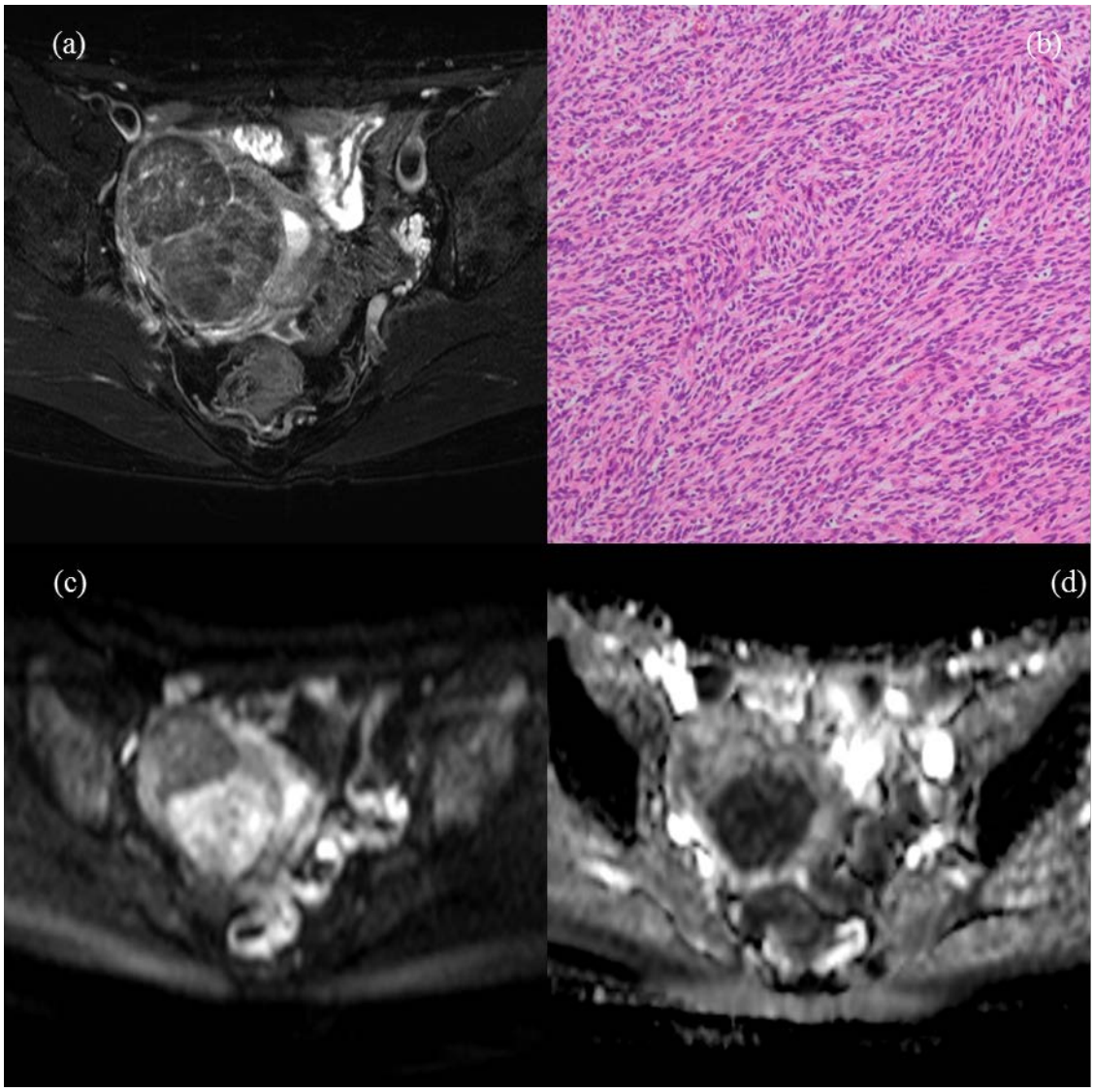


Figure7. : Group 3: Leiomyoma in a 62-year-old woman.

**a)** Axial T2WI showing a well-demarcated signal hypointense mass in the myometrium.

**c)** DWI with a b-value of 800 $mm^2/s$ showing high signal intensity on the dorsal aspect of the tumor.

**d)** ADC is 0.88 $\times 10^{-3}$ $mm^2/s$.

b) Hematoxylin and eosin-stained specimen. The cell density is 45.4%.

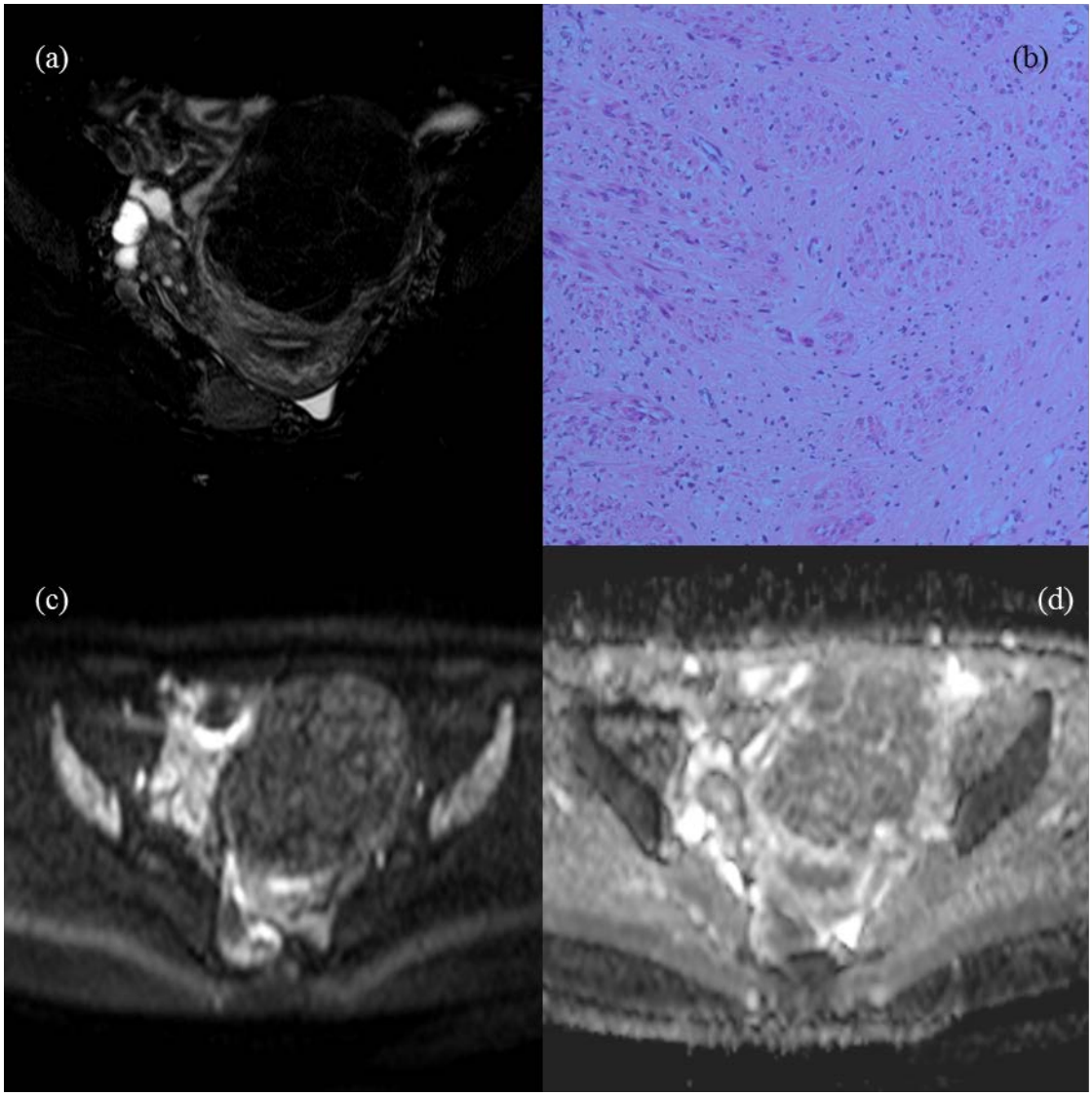


Figure8. : Group 4; Ordinary leiomyoma in a 42-year-old woman.

**a)** Axial T2WI showing a well-demarcated signal hypointense mass in the myometrium and subserosa.

**c)** DWI with a b-value of 800 $mm^2/s$ showing low signal intensity.

**d)** The ADC is 1.21 $\times 10^{-3}$ $mm^2/s$.

b) Hematoxylin and eosin-stained specimen. The cell density is 19.4%.